Commun. Optim. Theory 2023 (2023) 36 https://doi.org/10.23952/cot.2023.36

Communications in Optimization Theory
Available online at http://cot.mathres.org

A BOUNDARY OPERATOR APPROACH FOR THE SOLUTION OF A BIHARMONIC PROBLEM FROM INVERSE SOURCE PROBLEMS

ROLAND GLOWINSKI[1], DIANA ASSAELY LEÓN-VELASCO[2], LORENZO HÉCTOR JUÁREZ-VALENCIA[3,*], JOSÉ JULIO CONDE-MONES[4], JOSÉ JACOBO OLIVEROS-OLIVEROS[4]

[1]Department of Mathematics, University of Houston, USA; Department of Mathematics, Hong Kong Baptist, Hong Kong
[2]Departamento de Matemáticas Aplicadas y Sistemas, UAM-Cuajimalpa, México
[3]Departamento de Matemáticas, UAM-Iztapalapa, México
[4]Facultad de Ciencias Físico Matemáticas, Benemérita Universidad Autónoma de Puebla, México

Dedicated to the memory of Professor Roland Glowinski

Abstract. We discuss in this article a method for the numerical solution of a linear bi-harmonic problem arising from inverse source problems, like those in electroencephalography. In order to solve this bi-harmonic problem using low order Lagrange finite element approximations, we reformulate it as a functional equation associated with a linear boundary operator of the Steklov-Poincaré type. This boundary equation is well-suited to solution by a conjugate gradient algorithm, requiring the solution of two second order linear elliptic problems per iteration. The performance of our methodology is validated via the solution of test problems for simple and complex 2D geometries, disk-shaped domains in particular.

Keywords. Bi-harmonic problem; Conjugate gradient; Inverse electroencephalography; Linear boundary operator; low order finite elements.

2020 Mathematics Subject Classification. 78A46, 65C30.

1. Introduction

Our initial and main interest is the solution of an inverse source problem from measurements on the boundary of a bounded region. This problem is related to source sensing, from boundary data, in an electrical medium with piecewise constant conductivity. One important application corresponds with the inverse electroencephalography problem to recover sources that represent biolectrical activity of the brain (see [3], [30], [31], among others). A particular type of source

*Corresponding author.

E-mail address: roland@math.uh.edu (R. Glowinski), dleon@cua.uam.mx (D.A. León-Velasco), hect@xanum.uam.mx (L.H. Juárez-Valencia), jconden@fcfm.buap.mx (J.J. Conde-Mones), oliveros@fcfm.buap.mx (J.J. Oliveros-Oliveros).

Received: June 28, 2022; Accepted: April 26, 2023.

is a pointwise source to model epilepsy foci (see, e.g., [29] for further details). The EEG-measured neural activity from the brain can be described by a simplified two-layered Poisson's equation for electrical conduction (see [17], [35] and references therein):

$$-\nabla\cdot(\sigma\nabla y) = u|_{\Omega} \quad \text{in} \quad \mathfrak{D}, \tag{1.1}$$

$$\frac{\partial y}{\partial \mathbf{n}} = 0 \quad \text{on} \quad \partial\mathfrak{D}, \tag{1.2}$$

where y denotes the electrostatic potential, σ the conductivity, u the current sources in Ω (the region occupied by the brain), $\mathbf{n}$ the outward unit normal vector on the boundary $\partial\mathfrak{D}$ of the region occupied by the head (whose interior is denoted by $\mathfrak{D}$). Of course, the brain, represented by Ω, is a proper subdomain of $\mathfrak{D}$, which boundary we will denote by Γ. The inverse problem consist in finding an electrical source u acting on Ω from a given measured potential on the boundary of $\mathfrak{D}$:

$$y = y_d \quad \text{on} \quad \partial\mathfrak{D}. \tag{1.3}$$

If the only available information is the voltage y_d on $\partial\mathfrak{D}$, then only the harmonic component of the source u can be identified, and more information is needed to identify the complete source [15] and [3]. Therefore, we will assume that u belongs to the space

$$\mathscr{U} = \left\{v \mid v\in L^2(\Omega),\ \nabla^2 v = 0\right\}, \tag{1.4}$$

thus the above inverse problem for the identification of u can be formulated as a ***control problem for an elliptic equation***, namely:

$$\begin{cases} u\in\mathscr{U}, \\ J(u)\le J(v),\ \forall v\in\mathscr{U}, \end{cases} \tag{1.5}$$

where the functional $J:\mathscr{U}\to\mathbb{R}$ is defined by

$$J(v) = \frac{1}{2}\int_{\Omega}|v|^2 d\mathbf{x} + \frac{k}{2}\int_{\partial\mathfrak{D}}|y-y_d|^2 d\partial\mathfrak{D}, \tag{1.6}$$

where in (1.6): (a) The penalty parameter k is positive and large. (b) Function y_d is given typically in $L^\infty(\partial\mathfrak{D})$. (c) y is a function of v via the solution of the Neumann problem (1.1)-(1.2) whose variational formulation is given by

$$\begin{cases} y\in H^1(\mathfrak{D}), \\ \int_{\mathfrak{D}}\sigma\nabla y\cdot\nabla z\, d\mathbf{x} = \int_{\Omega} v z\, d\mathbf{x},\ \forall z\in H^1(\mathfrak{D}), \end{cases} \tag{1.7}$$

with $\sigma\in L^\infty(\mathfrak{D})$, $\sigma(x)\ge\sigma_0>0$, a.e. in $\mathfrak{D}$. The derivatives in (1.1)-(1.2), (1.4) and (1.7) are in the sense of distributions. Using the fact that $\mathscr{U}$ is a closed subspace of $L^2(\Omega)$ it is also a Hilbert space for the cannonical inner-product of $L^2(\Omega)$ and associated norm.

The minimization problem (1.5) has a unique solution, which can be computed by a ***conjugate gradient algorithm*** operating in the space $\mathscr{U}$, [22]. The implementation of this algorithm, or any other descent gradient algorithm, requires the knowledge of the differential $DJ(v)$ of J at v, $\forall v\in\mathscr{U}$. A simple perturbation analysis shows that

$$\delta J(v) = \int_{\Omega} DJ(v)\,\delta v\, d\mathbf{x},\ \forall\delta v\in\mathscr{U}, \tag{1.8}$$

with $DJ(v) \in \mathscr{U}$, and

$$\delta J(v) = \int_\Omega v\,\delta v\,d\mathbf{x} + k\int_{\partial\mathfrak{D}} (y - y_d)\,\delta y\,d\partial\mathfrak{D},\ \forall\,\delta v \in \mathscr{U}, \tag{1.9}$$

with δy a linear function of δv via the solution of

$$\begin{cases} \delta y \in H^1(\mathfrak{D}), \\ \displaystyle\int_{\mathfrak{D}} \sigma\nabla\delta y \cdot \nabla z\,d\mathbf{x} = \int_\Omega \delta v\,z\,d\mathbf{x},\ \forall z \in H^1(\mathfrak{D}). \end{cases} \tag{1.10}$$

Suppose that p verifies

$$\begin{cases} p \in H^1(\mathfrak{D}), \\ \displaystyle\int_{\mathfrak{D}} \sigma\nabla p \cdot \nabla z\,d\mathbf{x} = k\int_{\partial\mathfrak{D}} (y - y_d)\,z\,d\partial\mathfrak{D},\ \forall z \in H^1(\mathfrak{D}). \end{cases} \tag{1.11}$$

Combining relation (1.9) with (1.11), we obtain that

$$\int_\Omega DJ(v)\,\delta v\,d\mathbf{x} = \int_\Omega (v+p)\,\delta v\,d\mathbf{x},\ \forall\,\delta v \in \mathscr{U}, \tag{1.12}$$

which implies in turn that

$$\int_\Omega DJ(v)\,w\,d\mathbf{x} = \int_\Omega (v+p)\,w\,d\mathbf{x},\ \forall w \in \mathscr{U}. \tag{1.13}$$

We have thus shown that $DJ(v)$ is the $L^2(\Omega)$-orthogonal projection of the function $f = v + p|_\Omega$ on $\mathscr{U}$, a closed subspace of $L^2(\Omega)$. Although simple from a conceptual point of view, the projection from $L^2(\Omega)$ onto $\mathscr{U}$ is, computationally, a non-trivial operation.

Actually the numerical calculation of this projection leads to the solution of a bi-harmonic problem, as shown in Sect. 2. The numerical solution of this bi-harmonic problem is the main topic we want to discuss in this paper. For this purpose, we consider in Sect. 3 a boundary operator formulation of the bi-harmonic problem; we introduce in Sect. 4 a conjugate gradient (CG) algorithm in order to solve the above boundary operator equation; in Sect. 5 and 6 we consider the discretization of some elliptic subproblems arising in the CG algorithm; in Sect. 7.1 we consider some bi-harmonic problems with a closed form solution in a open disk, which are employed to validate the numerical methodology introduced in this article; in Sect. 7.2 we consider a numerical example in a complex 2D domain skull-shape related; finally, some conclusions are stated in Sect. 8.

The conjugate gradient solution of problem (1.5), and some related applications, will be addressed in a forthcoming separate article.

2. The biharmonic problem

Problem (1.13) is a linear variational problem, which is a particular case of

$$\begin{cases} f \in L^2(\Omega) \text{ being given, find } g \text{ solution of} \\ \begin{cases} g \in \mathscr{U}, \\ \displaystyle\int_\Omega g\,v\,d\mathbf{x} = \int_\Omega f\,v\,d\mathbf{x},\ \forall v \in \mathscr{U}. \end{cases} \end{cases} \tag{2.1}$$

Indeed (2.1) characterizes g as being the $L^2(\Omega)$-orthogonal projection of f on $\mathscr{U}$, a closed subspace of $L^2(\Omega)$; actually, it follows from (2.1) that $f - g \in \mathscr{U}^{\perp}$. Since

$$\mathscr{U}^{\perp} = \nabla^2 H_0^2(\Omega), \tag{2.2}$$

with $H_0^2(\Omega) = \{\varphi \,|\, \varphi \in H^2(\Omega),\, \varphi = 0,\, \partial\varphi/\partial\mathbf{n} = 0 \text{ on } \Gamma\} = \overline{\mathscr{D}(\Omega)}^{H^2(\Omega)}$ ($\mathscr{D}(\Omega)$ being the space of the C^∞ functions with compact support in Ω), then

$$f = (f - \nabla^2\psi) + \nabla^2\psi, \tag{2.3}$$

where $g = f - \nabla^2\psi$ and ψ is the unique solution in $H_0^2(\Omega)$ of the following bi-harmonic problem

$$\begin{aligned} \Delta^2\psi = \Delta f \quad & \text{in} \quad \Omega, \\ \psi = 0 \quad & \text{on} \quad \Gamma, \\ \frac{\partial\psi}{\partial\mathbf{n}} = 0 \quad & \text{on} \quad \Gamma, \end{aligned} \tag{2.4}$$

where $\Delta = \nabla^2$ is the Laplace operator and $\Gamma = \partial\Omega$. We emphasize that given $f \in L^2(\Omega)$ the solution of (2.1) in $\mathscr{U}$ is $g = f - \Delta\psi$ where ψ solves (2.4), and hereafter we will concentrate on the solution of this biharmonic problem.

A classical variational formulation of (2.4) is given by

$$\begin{cases} \psi \in H_0^2(\Omega), \\ \displaystyle\int_\Omega \Delta\psi\Delta\varphi\, d\mathbf{x} = \int_\Omega f\Delta\varphi\, d\mathbf{x}, \quad \forall\varphi \in H_0^2(\Omega). \end{cases} \tag{2.5}$$

Problem (2.4), (2.5), can be solved directly using classical numerical approximations. However, high order approximations are needed in order to deal with the high order derivatives in the equation. Actually, at present there are many different numerical methods and approaches in the literature that solve accurately the biharmonic equation, many of them are more popular or conventional than others. But, even though this equation is somehow classical, its numerical solution is still a topic of active research. For instance, in [1, 4, 5] spline collocation schemes are used to solve the problem in a rectangular domain or in on the unit square, while in [2, 6, 7, 18, 36] the biharmonic equation is solved with finite difference schemes on rectangular regions, also in [8, 28] finite differences schemes are employed but in a circular domain (using polar coordinates) and irregular domains, respectively. Other classical methods to solve the biharmonic problem in regular and irregular domains are finite element methods. For example, in [9, 12, 16, 23] the problem is solved using mixed finite elements, while discontinuous Galerkin and weak Galerkin finite elements are prefered in [13, 32, 33, 38]. Likewise, boundary integral equations methods have been also used extensively, as in [10, 11, 14, 19, 24, 25, 26, 27, 37]. The list of methods is really quite long and we have only mentioned some of the most common.

In this work, we will describe a method which is a close variant of one of the methods introduced in [23], where a linear boundary operator is employed to reformulate the biharmonic problem. The linear operator, being elliptical, allows to find the solution by a conjugate gradient algorithm with an ad-hoc preconditoner, requiring the solution of two second order linear elliptic problems per iteration. This approach is shown to be second order accurate, computationally cheap and well suited for simple and complex domains.

So, our main goal in this work is to introduce a reformulation of the problem which allows low order approximations, like linear finite elements, which are well suited for the numerical solution of second order elliptic problems on domains Ω of (almost) arbitrary shape. A way to make this possible is to observe that (2.4) is equivalent to the elliptic system:

$$\begin{aligned} \Delta\omega &= 0 \quad \text{in} \quad \Omega, \\ -\Delta\psi &= \omega - f \quad \text{in} \quad \Omega, \\ \psi &= 0 \quad \text{on} \quad \Gamma, \\ \frac{\partial\psi}{\partial\mathbf{n}} &= 0 \quad \text{on} \quad \Gamma. \end{aligned} \tag{2.6}$$

To solve problem (2.4), we are going to reduce the solution of (2.6) to the solution of a 'kind of' boundary integral equation associated with a symmetric strongly positive definite operator mapping $H^{-1/2}(\Gamma)$ onto $H^{1/2}(\Gamma)$. The idea is somehow introducing a functional boundary operator that relates the trace $\omega|_\Gamma$ to the normal derivative $\partial\psi/\partial\mathbf{n}$ in (2.6). This reduction will be discussed in Sect. 3 and 4.

3. Using (2.6) to reduce (2.4) to an operator equation in $H^{-1/2}(\Gamma)$

From (2.6), the function ω belongs clearly to the space $H(\Omega;\Delta) = \{\theta \,|\, \theta \in L^2(\Omega), \Delta\theta \in L^2(\Omega)\}$, an important property of the above space being (cf., [34]) that if $\theta \in H(\Omega;\Delta)$ then θ has a trace in $H^{-1/2}(\Gamma)$ and $\partial\theta/\partial\mathbf{n}$ exists in $H^{-3/2}(\Gamma)$. From these properties the function ω has a trace in $H^{-1/2}(\Gamma)$ that we will denote by λ. Consider now the solution ψ of problem (2.4); we observe that

$$\psi = \psi_\lambda + \psi_0, \tag{3.1}$$

where ψ_λ and ψ_0 are the respective solutions of

$$\begin{cases} -\Delta\psi_\lambda = \omega \text{ in } \Omega, \\ \psi_\lambda = 0 \text{ on } \Gamma, \end{cases} \tag{3.2}$$

and

$$\begin{cases} \Delta\psi_0 = f \text{ in } \Omega, \\ \psi_0 = 0 \text{ on } \Gamma. \end{cases} \tag{3.3}$$

We have thus

$$-\frac{\partial\psi_\lambda}{\partial\mathbf{n}} = \frac{\partial\psi_0}{\partial\mathbf{n}} \text{ on } \Gamma. \tag{3.4}$$

Let us define an operator A mapping $H^{-1/2}(\Gamma)$ into $H^{1/2}(\Gamma)$ by

$$A\mu = -\frac{\partial\psi_\mu}{\partial\mathbf{n}}, \tag{3.5}$$

where ψ_μ is obtained from μ via the solution of

$$\begin{cases} \Delta\omega_\mu = 0 \text{ in } \Omega, \\ \omega_\mu = \mu \text{ on } \Gamma, \end{cases} \tag{3.6}$$

and

$$\begin{cases} -\Delta\psi_\mu = \omega_\mu \text{ in } \Omega, \\ \psi_\mu = 0 \text{ on } \Gamma. \end{cases} \tag{3.7}$$

Operator A is *continuous*, *self-adjoint* and *positive definite*. Indeed, let us consider μ_1 and μ_2 belonging to $H^{-1/2}(\Gamma)$; we have then, with obvious notation

$$\int_\Gamma \frac{\partial \psi_1}{\partial \mathbf{n}} \mu_2 \, d\Gamma = \int_\Gamma \frac{\partial \psi_1}{\partial \mathbf{n}} \omega_2 \, d\Gamma = \int_\Gamma \frac{\partial \omega_2}{\partial \mathbf{n}} \psi_1 \, d\Gamma + \int_\Omega (\Delta\psi_1 \, \omega_2 - \Delta\omega_2 \, \psi_1) \, d\mathbf{x} = -\int_\Omega \omega_1 \omega_2 \, d\mathbf{x}, \tag{3.8}$$

for all $\mu_1, \mu_2 \in H^{-1/2}(\Gamma)$.

Remark 3.1. For mathematical rigor, the boundary integrals in (3.8) should be replaced by appropriate duality pairings.

It follows from (3.8) that

$$\langle A\mu_1, \mu_2 \rangle = \int_\Omega \omega_1 \, \omega_2 \, d\mathbf{x}, \quad \forall \mu_1, \mu_2 \in H^{-1/2}(\Gamma), \tag{3.9}$$

where in (3.9), $\langle \cdot, \cdot \rangle$ denotes the duality pairing between $H^{-1/2}(\Gamma)$ and $H^{1/2}(\Gamma)$, which coincides with the $L^2(\Gamma)$–inner product if the second argument is smooth enough. Relation (3.9) implies that A is self-adjoint and positive semi-definite. Operator A is also positive definite since, from (3.9),

$$\langle A\mu, \mu \rangle = 0 \quad \Rightarrow \quad \int_\Omega |\omega_\mu|^2 dx = 0 \quad \Rightarrow \quad \omega_\mu = 0 \quad \Rightarrow \quad \mu = \omega_\mu|_\Gamma = 0.$$

Actually, since the bi-harmonic problem

$$\begin{cases} \Delta^2 \Phi = 0 \text{ in } \Omega, \\ \Phi = 0 \text{ on } \Gamma, \quad \dfrac{\partial \Phi}{\partial \mathbf{n}} = \phi \text{ on } \Gamma, \end{cases} \tag{3.10}$$

has a (unique) solution in $H^2(\Omega) \cap H_0^1(\Omega)$, $\forall \phi \in H^{1/2}(\Gamma)$, operator A is an isomorphism (algebraically and topologically) from $H^{-1/2}(\Gamma)$ onto $H^{1/2}(\Gamma)$. Operator A is clearly of the Steklov-Poincaré type.

Back to problem (2.6), the above results imply that the trace λ of ω on Γ is the unique solution of the functional equation

$$\boxed{A\lambda = \frac{\partial \psi_0}{\partial \mathbf{n}}}. \tag{3.11}$$

It has been shown in [23] that if Ω is a disk, then A is a boundary integral operator whose kernel is known explicitly.

A variational formulation of (3.11) is given by

$$\begin{cases} \lambda \in H^{-1/2}(\Gamma), \\ \langle A\lambda, \mu \rangle = \left\langle \dfrac{\partial \psi_0}{\partial \mathbf{n}}, \mu \right\rangle, \quad \forall \mu \in H^{-1/2}(\Gamma), \end{cases} \tag{3.12}$$

where in (3.12), $\langle \cdot, \cdot \rangle$ denotes the duality pairing between $H^{-1/2}(\Gamma)$ and $H^{1/2}(\Gamma)$ which reduces to the $L^2(\Gamma)$–inner product if the second argument is smooth enough.

Summarizing, we remember that the solution of the biharmonic problem is of the form (3.1) where ψ_0 solves (3.3) and ψ_λ solves (3.2), ω being the solution of (3.6) with $\mu = \lambda$. Taking advantage that operator A is self-adjoint and positive definite, we compute λ with a preconditioned conjugate gradient algorithm, which is described in the next section.

4. On the solution of problem (3.11), (3.12) by a conjugate gradient algorithm operating in $H^{-1/2}(\Gamma)$

4.1. **Some preliminary considerations.** Let S denotes a self–adjoint continuous linear operator from $H^{-1/2}(\Gamma)$ into $H^{1/2}(\Gamma)$. We suppose that operator S is strongly elliptic in the sense that $\exists\,\alpha > 0$, such that $\langle S\mu,\mu\rangle \geq \alpha\|\mu\|^2_{H^{-1/2}(\Gamma)}$, $\forall\,\mu \in H^{-1/2}(\Gamma)$; in fact, operator S is an isomorphism from $H^{-1/2}(\Gamma)$ onto $H^{1/2}(\Gamma)$. Actually, it follows from the above properties of S that the bilinear functional $\{\mu_1,\mu_2\} \to \langle S\mu_1,\mu_2\rangle$ defines over $H^{-1/2}(\Gamma)$ an inner–product whose associated norm is equivalent to $\|\cdot\|_{H^{-1/2}(\Gamma)}$. Below, we are going to solve problem (2.6) using a conjugate gradient algorithm operating in $H^{-1/2}(\Gamma)$ equipped with the inner–product and norm associated with operator S, as described above.

It is important to notice that the linear operator S is introduced here with the idea of describing a preconditioned conjugate gradient algorithm in a general manner. The concrete form of the preconditoner is introduced in the next subsection.

4.2. **Description of the conjugate gradient algorithm.** Following [20] (Chapters 3 & 10) and [21] (Chapter 2), the conjugate gradient algorithm we intend to use for the solution of problem (3.11), (3.12) reads as follows:

$$\lambda^0 \text{ is given in } H^{-1/2}(\Gamma)\ (\lambda^0 = 0\text{, e.g., but smarter choices may be available}). \tag{4.1}$$

Solve the following elliptic system in $H(\Omega;\Delta)\times H^1_0(\Omega)$:

$$\begin{cases} \Delta\omega^0 = 0 \text{ in } \Omega, \\ \omega^0 = \lambda^0 \text{ on } \Gamma, \end{cases} \tag{4.2}$$

$$\begin{cases} -\Delta\psi^0 = \omega^0 - f \text{ in } \Omega, \\ \psi^0 = 0 \text{ on } \Gamma. \end{cases} \tag{4.3}$$

Solve next

$$\begin{cases} g^0 \in H^{-1/2}(\Gamma), \\ \langle Sg^0,\mu\rangle = -\left\langle \dfrac{\partial\psi^0}{\partial\mathbf{n}},\mu\right\rangle, \forall\mu \in H^{-1/2}(\Gamma). \end{cases} \tag{4.4}$$

If $\dfrac{\langle Sg^0,g^0\rangle}{\max[1,\langle S\lambda^0,\lambda^0\rangle]} \leq tol$ take $\lambda = \lambda^0$; otherwise, set

$$w^0 = g^0. \tag{4.5}$$

For $n \geq 0$, λ^n, g^n, w^n being known, the last two different from 0, compute λ^{n+1}, g^{n+1} and if necessary w^{n+1} as follows:

Solve the following elliptic system in $H(\Omega;\Delta)\times H^1_0(\Omega)$:

$$\begin{cases} \Delta\overline{\omega}^n = 0 \text{ in } \Omega, \\ \overline{\omega}^n = w^n \text{ on } \Gamma, \end{cases} \tag{4.6}$$

$$\begin{cases} -\Delta\overline{\psi}^n = \overline{\omega}^n \text{ in } \Omega, \\ \overline{\psi}^n = 0 \text{ on } \Gamma. \end{cases} \tag{4.7}$$

Solve next

$$\begin{cases} \overline{g}^n \in H^{-1/2}(\Gamma), \\ \langle S\overline{g}^n, \mu \rangle = -\left\langle \dfrac{\partial \overline{\psi}^n}{\partial \mathbf{n}}, \mu \right\rangle, \forall \mu \in H^{-1/2}(\Gamma), \end{cases} \tag{4.8}$$

and compute

$$\rho_n = \frac{\langle Sg^n, g^n \rangle}{\langle S\overline{g}^n, w^n \rangle}, \tag{4.9}$$

$$\lambda^{n+1} = \lambda^n - \rho_n w^n, \tag{4.10}$$

$$g^{n+1} = g^n - \rho_n \overline{g}^n. \tag{4.11}$$

If $\dfrac{\langle Sg^{n+1}, g^{n+1} \rangle}{\max[\langle Sg^0, g^0 \rangle, \langle S\lambda^{n+1}, \lambda^{n+1} \rangle]} \leq tol$ take $\lambda = \lambda^0$; otherwise, compute

$$\gamma_n = \frac{\langle Sg^{n+1}, g^{n+1} \rangle}{\langle Sg^n, g^n \rangle}, \tag{4.12}$$

$$w^{n+1} = g^{n+1} + \gamma_n w^n. \tag{4.13}$$

Do $n+1 \to n$ and return to (4.6).

4.3. **A possible choice for operator S.** With κ a positive number let us define the boundary operator B acting on $H^{1/2}(\Gamma)$ by

$$B\mu = \mu + \kappa \frac{\partial \theta_\mu}{\partial \mathbf{n}}, \quad \forall \mu \in H^{1/2}(\Gamma), \tag{4.14}$$

where θ_μ is the unique solution in $H^1(\Omega)$ of the following Laplace–Dirichlet problem:

$$\begin{cases} \Delta \theta_\mu = 0 \text{ in } \Omega, \\ \theta_\mu = \mu \text{ on } \Gamma. \end{cases} \tag{4.15}$$

We have then $\partial \theta_\mu / \partial \mathbf{n} \in H^{-1/2}(\Gamma)$ and (with obvious notation) the relation

$$\begin{aligned} \langle B\mu_1, \mu_2 \rangle &= \int_\Gamma \mu_1 \mu_2 \, d\Gamma + \kappa \left\langle \frac{\partial \theta_1}{\partial \mathbf{n}}, \mu_2 \right\rangle \\ &= \int_\Gamma \theta_1 \theta_2 \, d\Gamma + \kappa \int_\Omega \nabla \theta_1 \cdot \nabla \theta_2 \, d\mathbf{x}, \ \ \forall \mu_1, \mu_2 \in H^{1/2}(\Gamma), \end{aligned} \tag{4.16}$$

implying that operator B is a strongly elliptic self–adjoint isomorphism from $H^{1/2}(\Gamma)$ onto $H^{-1/2}(\Gamma)$. On the other hand, the operator S defined by

$$S = B^{-1} \tag{4.17}$$

is a strongly elliptic self–adjoint isomorphism from $H^{-1/2}(\Gamma)$ onto $H^{1/2}(\Gamma)$, implying that the bilinear functional

$$\{\mu_1, \mu_2\} \longrightarrow \langle S\mu_1, \mu_2 \rangle \tag{4.18}$$

defines an inner–product over $H^{-1/2}(\Gamma)$ and therefore, can be used in algorithm (4.1)–(4.13), as shown in Sect. 4.4, here after.

4.4. **Description of the conjugate gradient algorithm (4.1)-(4.13) when operator S is defined by (4.14)-(4.17).** If operator S is defined by (4.14)-(4.17), a more detailed description of the conjugate gradient algorithm (4.1)-(4.13) is given by:

$$\lambda^0 \text{ is given in } H^{-1/2}(\Gamma). \tag{4.19}$$

Solve the following elliptic system in $H(\Omega;\Delta)\times H_0^1(\Omega)$:

$$\begin{cases} \Delta\omega^0 = 0 \text{ in } \Omega, \\ \omega^0 = \lambda^0 \text{ on } \Gamma, \end{cases} \tag{4.20}$$

$$\begin{cases} -\Delta\psi^0 = \omega^0 - f \text{ in } \Omega, \\ \psi^0 = 0 \text{ on } \Gamma. \end{cases} \tag{4.21}$$

Next, define $r^0 \in H^{1/2}(\Gamma)$ by

$$r^0 = -\frac{\partial\psi^0}{\partial\mathbf{n}}, \tag{4.22}$$

and θ^0 as the unique solution in $H^1(\Omega)$ of

$$\begin{cases} \Delta\theta^0 = 0 \text{ in } \Omega, \\ \theta^0 = r^0 \text{ on } \Gamma. \end{cases} \tag{4.23}$$

Set

$$g^0 = r^0 + \kappa\frac{\partial\theta^0}{\partial\mathbf{n}}. \tag{4.24}$$

If $\dfrac{\langle r^0, g^0\rangle}{\max[1,\langle S\lambda^0,\lambda^0\rangle]} \le tol$ take $\lambda = \lambda^0$; otherwise, set

$$w^0 = g^0. \tag{4.25}$$

For $n \ge 0$, λ^n, r^n, g^n, w^n being known, the three different from 0, compute λ^{n+1}, r^{n+1}, g^{n+1} and if necessary w^{n+1} as follows:

Solve the following elliptic system in $H(\Omega;\Delta)\times H_0^1(\Omega)$:

$$\begin{cases} \Delta\overline{\omega}^n = 0 \text{ in } \Omega, \\ \overline{\omega}^n = w^n \text{ on } \Gamma, \end{cases} \tag{4.26}$$

$$\begin{cases} -\Delta\overline{\psi}^n = \overline{\omega}^n \text{ in } \Omega, \\ \overline{\psi}^n = 0 \text{ on } \Gamma. \end{cases} \tag{4.27}$$

Next, define $\overline{r}^n \in H^{1/2}(\Gamma)$ by

$$\overline{r}^n = -\frac{\partial\overline{\psi}^n}{\partial\mathbf{n}}, \tag{4.28}$$

and $\overline{\theta}^n$ as the unique solution in $H^1(\Omega)$ of

$$\begin{cases} \Delta\overline{\theta}^n = 0 \text{ in } \Omega, \\ \overline{\theta}^n = \overline{r}^n \text{ on } \Gamma. \end{cases} \tag{4.29}$$

Set

$$\overline{g}^n = \overline{r}^n + \kappa \frac{\partial \overline{\theta}^n}{\partial \mathbf{n}}. \tag{4.30}$$

Compute

$$\rho_n = \frac{\langle r^n, g^n \rangle}{\langle \overline{r}^n, w^n \rangle}, \tag{4.31}$$

$$\lambda^{n+1} = \lambda^n - \rho_n w^n, \tag{4.32}$$

$$r^{n+1} = r^n - \rho_n \overline{r}^n, \tag{4.33}$$

$$g^{n+1} = g^n - \rho_n \overline{g}^n. \tag{4.34}$$

If $\dfrac{\langle r^{n+1}, g^{n+1} \rangle}{\max[\langle r^0, g^0 \rangle, \langle S\lambda^{n+1}, \lambda^{n+1} \rangle]} \leq tol$ take $\lambda = \lambda^{n+1}$; otherwise, compute

$$\gamma_n = \frac{\langle r^{n+1}, g^{n+1} \rangle}{\langle r^n, g^n \rangle}, \tag{4.35}$$

$$w^{n+1} = g^{n+1} + \gamma_n w^n. \tag{4.36}$$

Do $n+1 \to n$ and return to (4.26).

The *finite element* implementation of algorithm (4.19)-(4.36) will be discussed below.

5. A MIXED FINITE ELEMENT APPROXIMATION OF PROBLEM (2.4)

5.1. **Some preliminary results.** Following [23] (see also [20], Chapter 10) we are going to approximate the bi-harmonic problem (2.4) by a mixed finite element method making the implementation of algorithm (4.19)-(4.36) relatively straightforward. Our starting point will be the equivalent formulation (2.6) of problem (2.4), that is

$$\begin{aligned} \Delta\omega &= 0 \quad \text{in} \quad \Omega, \\ -\Delta\psi &= \omega - f \quad \text{in} \quad \Omega, \\ \psi = 0,\ \frac{\partial \psi}{\partial \mathbf{n}} &= 0 \quad \text{on} \quad \Gamma. \end{aligned} \tag{5.1}$$

It is worth noticing that (5.1) implies (from the 1$^{\text{st}}$ Green's formula):

$$\frac{\partial \psi}{\partial \mathbf{n}} = 0 \iff \int_\Omega (f-\omega)\,\varphi\, d\mathbf{x} + \int_\Omega \nabla\psi \cdot \nabla\varphi\, d\mathbf{x} = 0, \quad \forall\ \varphi \in H^1(\Omega). \tag{5.2}$$

Relation (5.2) and its discrete analogues will play a most useful role hereafter.

5.2. **The fundamental discrete spaces.** Let assume that Ω is a bounded polygonal of $\mathbb{R}^2$ and that $\mathscr{T}_h$ is a triangulation of Ω verifying those classical assumptions listed in, e.g., [20] (Appendix 1) and [21] (Chapter 1). Among them, the facts that all the triangles of $\mathscr{T}_h$ are closed and that $\cup_{T\in\mathscr{T}_h} = \overline{\Omega}$. From $\mathscr{T}_h$ we approximate $H^1(\Omega)$ and $H^1_0(\Omega)$ by

$$V_h = \{\varphi \,|\, \varphi \in C^0(\overline{\Omega}),\ \varphi|_T \in P_1, \forall T \in \mathscr{T}_h\}, \tag{5.3}$$

and

$$V_{0h} = \{\varphi \,|\, \varphi \in V_h,\ \varphi|_\Gamma = 0\}, \tag{5.4}$$

respectively, with P_1 the space of the two–variable polynomials of degree ≤ 1. The following subspace of V_h will be particularly useful concerning the approximation of problem (3.11), (3.12) and its solution by either direct or iterative methods:

$$M_h = \{\varphi \,|\, \varphi \in V_h,\, \varphi|_T = 0, \forall T \in \mathscr{T}_h, \partial T \cap \Gamma = \emptyset\}. \tag{5.5}$$

We clearly have

$$V_h = V_{0h} \oplus M_h, \tag{5.6}$$

and (of course)

$$\dim(M_h) = \dim(V_h) - \dim(V_{0h}).$$

Actually, $\dim(M_h)$ is equal to the number of vertices of $\mathscr{T}_h$ located on Γ.

5.3. **On several approximations of problem (5.1).** We approximate problem (5.1) by

$$\begin{cases} \{\omega_h, \psi_h\} \in V_h \times V_{0h}, \\ \int_\Omega \nabla\omega_h \cdot \nabla\varphi \, d\mathbf{x} = 0, \quad \forall\, \varphi \in V_{0h}, \\ \int_\Omega \nabla\psi_h \cdot \nabla\varphi \, d\mathbf{x} = \int_\Omega (\omega_h - f_h)\varphi \, d\mathbf{x}, \quad \forall\, \varphi \in V_{0h}, \\ \int_\Omega \nabla\psi_h \cdot \nabla\mu \, d\mathbf{x} + \int_\Omega (f_h - \omega_h)\mu \, d\mathbf{x} = 0, \quad \forall\, \mu \in M_h, \end{cases} \tag{5.7}$$

where, in (5.7), f_h is an approximation of f belonging to V_h. In order to solve (5.7), we are going to take advantage of its equivalence with

$$\begin{cases} \{\lambda_h, \omega_h, \psi_h\} \in M_h \times V_h \times V_{0h}, \\ \begin{cases} \omega_h - \lambda_h \in V_{0h}, \\ \int_\Omega \nabla\omega_h \cdot \nabla\varphi \, d\mathbf{x} = 0, \quad \forall\, \varphi \in V_{0h}, \end{cases} \\ \int_\Omega \nabla\psi_h \cdot \nabla\varphi \, d\mathbf{x} = \int_\Omega (\omega_h - f_h)\varphi \, d\mathbf{x}, \quad \forall\, \varphi \in V_{0h}, \\ \int_\Omega \nabla\psi_h \cdot \nabla\mu \, d\mathbf{x} + \int_\Omega (f_h - \omega_h)\mu \, d\mathbf{x} = 0, \quad \forall\, \mu \in M_h, \end{cases} \tag{5.8}$$

where λ_h is nothing but the component of ω_h in M_h according to the decomposition (5.6) of the space V_h; function λ_h will play for the discrete bi–harmonic problem the role played by the trace λ of ω for the continuous one. Relations (5.8) imply that λ_h is the unique solution of the following linear variational problem in M_h:

$$\begin{cases} \lambda_h \in M_h, \\ a_h(\lambda_h, \mu) = L_h(\mu), \quad \forall\, \mu \in M_h, \end{cases} \tag{5.9}$$

where, in (5.9), the bilinear functional $a_h(\lambda_h, \mu)$ and the linear functional $L_h(\cdot)$ are defined, respectively, by:

(i)

$$a_h(\mu_1, \mu_2) = -\int_\Omega \nabla\psi_1 \cdot \nabla\mu_2 \, d\mathbf{x} + \int_\Omega \omega_1 \mu_2 \, d\mathbf{x}, \quad \forall\, \mu_1, \mu_2 \in M_h, \tag{5.10}$$

with, $\forall\, i = 1, 2$, ω_i and ψ_i uniquely defined by

$$\begin{cases} \omega_i - \mu_i \in V_{0h}, \\ \int_\Omega \nabla\omega_i \cdot \nabla\varphi \, d\mathbf{x} = 0, \quad \forall\, \varphi \in V_{0h}, \end{cases} \tag{5.11}$$

and

$$\begin{cases} \psi_i \in V_{0h}, \\ \displaystyle\int_\Omega \nabla \psi_i \cdot \nabla \varphi \, d\mathbf{x} - \int_\Omega \omega_i \, \varphi \, d\mathbf{x} = 0, \quad \forall \varphi \in V_{0h}. \end{cases} \tag{5.12}$$

(ii)

$$L_h(\mu) = \int_\Omega \nabla \psi_{0h} \cdot \nabla \mu \, d\mathbf{x} + \int_\Omega f_h \, \mu \, d\mathbf{x}, \quad \forall \mu \in M_h, \tag{5.13}$$

with ψ_{0h} the unique solution of

$$\begin{cases} \psi_{0h} \in V_{0h}, \\ \displaystyle\int_\Omega \nabla \psi_{0h} \cdot \nabla \varphi \, d\mathbf{x} = -\int_\Omega f_h \varphi \, d\mathbf{x}, \quad \forall \varphi \in V_{0h}. \end{cases} \tag{5.14}$$

We can easily prove that the above relations imply that

$$a_h(\mu_1, \mu_2) = \int_\Omega \omega_1 \, \omega_2 \, d\mathbf{x}, \quad \forall \mu_1, \mu_2 \in M_h, \tag{5.15}$$

which implies in turn that the bilinear functional $a_h(\cdot,\cdot)$ is ***symmetric*** and ***positive definite*** over $M_h \times M_h$. From these properties, problem (5.9) can be solved by a ***conjugate gradient algorithm*** operating in M_h; such an algorithm will be discussed in Sect. 6.3, hereafter.

Remark 5.1. Above, all the $L^2(\Omega)$–inner products have been computed exactly. A computer friendlier alternative is obtained by approximating all the integrals of the form

$$\int_\Omega \theta \, \varphi \, d\mathbf{x}, \quad \forall \theta, \varphi \in V_h \tag{5.16}$$

using the ***trapezoidal rule***. We obtain then the following approximation of (5.16):

$$\frac{1}{3} \sum_{Q \in \Sigma_h} |\overline{\Omega}_Q| \, \theta(Q) \, \varphi(Q), \quad \forall \theta, \varphi \in V_h, \tag{5.17}$$

where in (5.17): (i) Σ_h is the set of all the vertices of $\mathscr{T}_h$, (ii) $\overline{\Omega}_Q$ is the polygonal union of those triangles of $\mathscr{T}_h$ which have Q has a common vertex, (iii) $|\overline{\Omega}_Q| = \text{measure}(\overline{\Omega}_Q)$.

6. On the solution of problem (5.9)

6.1. **Generalities.** If the solution λ_h of problem (5.9) is known, obtaining the solution $\{\omega_h, \psi_h\}$ of problem (5.7) is a trivial matter since it requires the solution of two discrete Poisson problems. Solving such discrete problems being routine nowadays, we will focus on the solution of problem (5.9), a discrete variant of the boundary equation (3.11). Following [23] and [20], two classes of solution methods will be discussed, namely: (i) In Sect. 6.2 a *quasi–direct method* (as called in [23]), which may be of interest for those situations where many problems (2.4), differing only by f have to be solved. (ii) In Sect. 6.3, a ***preconditioned conjugate gradient*** algorithm (discrete variant of algorithm (4.19)-(4.36)).

6.2. **A quasi–direct method.** Let $\sigma_h = \{Q_j\}_{j=1}^J$ be the set of the vertices of $\mathscr{T}_h$ located on Γ; we have then dim(M_h)= J. Next, with every $Q_j \in \sigma_h$, we associate the shape function w_j uniquely defined by

$$\begin{cases} w_j \in V_h, \\ w_j(Q_j) = 1; w_j(Q) = 0, \ \forall Q \text{ vertex of } \mathscr{T}_h, \ Q \neq Q_j. \end{cases} \tag{6.1}$$

The set $\{w_j\}_{j=1}^J$ is clearly a vector basis of M_h. Let us return to the linear variational problem (5.9): assuming that

$$\lambda^n = \sum_{j=1}^J \lambda_j w_j, \tag{6.2}$$

problem (5.9) is equivalent to the following linear system

$$\sum_{j=1}^J a_h(w_j, w_i) = L_h(w_i), \quad 1 \leq i \leq J. \tag{6.3}$$

The matrix $(a_h(w_j, w_i))_{1\leq i,j\leq J}$ being symmetric and positive definite, its Cholesky factors can be computed once for all. The computation of the above matrix coefficients and of the right hand sides takes advantage of relations (5.10) and (5.13) which imply with obvious notation that:

(i)

$$a_h(w_j, w_i) = -\int_\Omega \nabla\psi_j \cdot \nabla w_i \, d\mathbf{x} + \int_\Omega \omega_j w_i \, d\mathbf{x}, \tag{6.4}$$

with, ω_j and ψ_j uniquely defined by

$$\begin{cases} \omega_j - w_j \in V_{0h}, \\ \displaystyle\int_\Omega \nabla\omega_j \cdot \nabla\varphi \, d\mathbf{x} = 0, \quad \forall \varphi \in V_{0h}, \end{cases} \tag{6.5}$$

and

$$\begin{cases} \psi_j \in V_{0h}, \\ \displaystyle\int_\Omega \nabla\psi_j \cdot \nabla\varphi \, d\mathbf{x} = \int_\Omega \omega_j \varphi \, d\mathbf{x}, \quad \forall \varphi \in V_{0h}. \end{cases} \tag{6.6}$$

An alternative to (6.4) is provided by

$$a_h(w_j, w_i) = \int_\Omega \omega_j \omega_i \, d\mathbf{x}, \tag{6.7}$$

(ii)

$$L(w_i) = \int_\Omega \nabla\psi_{0h} \cdot \nabla w_i \, d\mathbf{x} + \int_\Omega f_h w_i \, d\mathbf{x}. \tag{6.8}$$

We observe that the integrals in (6.4) and (6.8) (or their trapezoidal approximations) are simple to compute since they have to be evaluated on the support of the function w_i, that is on the polygonal Ω_{Q_i}. We observe also that the symmetry of matrix $(a_h(w_j, w_i))_{1\leq i,j\leq J}$ reduces the computational work necessary to construct it.

6.3. **On the conjugate gradient solution of problem (5.9).** An alternative to the quasi–direct solution method discussed in Section 6.2 is provided by the following discrete variant of algorithm (4.19)–(4.36):

$$\lambda_0 \text{ is given in } M_h. \tag{6.9}$$

Solve the following discrete elliptic system in $V_h \times V_{0h}$:

$$\begin{cases} \omega^0 - \lambda^0 \in V_{0h}, \\ \displaystyle\int_\Omega \nabla\omega^0 \cdot \nabla\varphi\, d\mathbf{x} = 0, \quad \forall\, \varphi \in V_{0h}, \end{cases} \tag{6.10}$$

$$\begin{cases} \psi^0 \in V_{0h}, \\ \displaystyle\int_\Omega \nabla\psi^0 \cdot \nabla\varphi\, d\mathbf{x} = \int_\Omega (\omega^0 - f_h)\,\varphi\, d\mathbf{x}, \quad \forall\, \varphi \in V_{0h}. \end{cases} \tag{6.11}$$

Next, define r^0 by

$$\begin{cases} r^0 \in M_h, \\ \displaystyle\int_\Omega r^0 \mu\, d\mathbf{x} = -\int_\Omega \nabla\psi^0 \cdot \nabla\mu\, d\mathbf{x} + \int_\Omega (\omega^0 - f_h)\,\mu\, d\mathbf{x}, \quad \forall\, \mu \in M_h, \end{cases} \tag{6.12}$$

and θ^0 as the unique solution in V_h of

$$\begin{cases} \theta^0 - r^0 \in V_{0h}, \\ \displaystyle\int_\Omega \nabla\theta^0 \cdot \nabla\varphi\, d\mathbf{x} = 0, \quad \forall\, \varphi \in V_{0h}. \end{cases} \tag{6.13}$$

Compute g^0 via the solution of

$$\begin{cases} g^0 - r^0 \in M_h, \\ \displaystyle\int_\Omega (g^0 - r^0)\,\mu\, d\mathbf{x} = \kappa \int_\Omega \nabla\theta^0 \cdot \nabla\mu\, d\mathbf{x}, \quad \forall\, \mu \in M_h. \end{cases} \tag{6.14}$$

If $\dfrac{\displaystyle\int_\Omega r^0 g^0\, d\mathbf{x}}{\max[1, a_h(\lambda^0, \lambda^0)]} \leq tol$ take $\lambda = \lambda^0$; otherwise, set

$$w^0 = g^0. \tag{6.15}$$

For $n \geq 0$, λ^n, r^n, g^n, w^n being known, the last three different from 0, compute λ^{n+1}, r^{n+1}, g^{n+1} and if necessary w^{n+1} as follows:
Solve the following discrete elliptic system in $V_h \times V_{0h}$:

$$\begin{cases} \overline{\omega}^n - w^n \in V_{0h}, \\ \displaystyle\int_\Omega \nabla\overline{\omega}^n \cdot \nabla\varphi\, d\mathbf{x} = 0, \quad \forall\, \varphi \in V_{0h}, \end{cases} \tag{6.16}$$

$$\begin{cases} \overline{\psi}^n \in V_{0h}, \\ \displaystyle\int_\Omega \nabla\overline{\psi}^n \cdot \nabla\varphi\, d\mathbf{x} = \int_\Omega \overline{\omega}^n\,\varphi\, d\mathbf{x}, \quad \forall\, \varphi \in V_{0h}. \end{cases} \tag{6.17}$$

Next, define $\overline{r}^n$ by

$$\begin{cases} \overline{r}^n \in M_h, \\ \displaystyle\int_\Omega \overline{r}^n \mu\, d\mathbf{x} = -\int_\Omega \nabla\overline{\psi}^n \cdot \nabla\mu\, d\mathbf{x} + \int_\Omega \overline{\omega}^n\,\mu\, d\mathbf{x}, \quad \forall\, \mu \in M_h, \end{cases} \tag{6.18}$$

and $\overline{\theta}^n \in V_h$ as the unique solution of

$$\begin{cases} \overline{\theta}^n - \overline{r}^n \in V_{0h}, \\ \int_\Omega \nabla \overline{\theta}^n \cdot \nabla \varphi \, d\mathbf{x} = 0, \quad \forall \varphi \in V_{0h}. \end{cases} \tag{6.19}$$

Compute $\overline{g}^n \in M_h$ as the solution of

$$\begin{cases} \overline{g}^n \in M_h, \\ \int_\Omega (\overline{g}^n - \overline{r}^n)\, \mu \, d\mathbf{x} = \kappa \int_\Omega \nabla \overline{\theta}^n \cdot \nabla \mu \, d\mathbf{x} = 0, \quad \forall \mu \in M_h, \end{cases} \tag{6.20}$$

and then

$$\rho_n = \frac{\int_\Omega r^n g^n \, d\mathbf{x}}{\int_\Omega \overline{r}^n w^n \, d\mathbf{x}}, \tag{6.21}$$

$$\lambda^{n+1} = \lambda^n - \rho_n w^n, \tag{6.22}$$

$$r^{n+1} = r^n - \rho_n \overline{r}^n, \tag{6.23}$$

$$g^{n+1} = g^n - \rho_n \overline{g}^n. \tag{6.24}$$

If $\dfrac{\int_\Omega r^{n+1} g^{n+1} \, d\mathbf{x}}{\max\left[\int_\Omega r^0 g^0 \, d\mathbf{x},\, a_h(\lambda^{n+1}, \lambda^{n+1})\right]} \leq tol$ take $\lambda = \lambda^0$; otherwise, compute

$$\gamma_n = \frac{\int_\Omega r^{n+1} g^{n+1} \, d\mathbf{x}}{\int_\Omega r^n g^n \, d\mathbf{x}}, \tag{6.25}$$

$$w^{n+1} = g^{n+1} + \gamma_n w^n. \tag{6.26}$$

Do $n+1 \to n$ and return to (6.16).

Actually, if discrete elliptic solvers are available the implementation of algorithm (6.9)-(6.26) is not that complicated, particularly if taking advantage of Sect. 5.1, we use (5.17) to replace all the integrals of the (5.16) type. The only delicate matter left to address is the calculation of the quantities $a_h(\lambda^0, \lambda^0)$ and $a_h(\lambda^{n+1}, \lambda^{n+1})$ occurring in the stopping criteria. Since $\lambda^{n+1} = \lambda^n - \rho_n w^n$, we have

$$a_h(\lambda^{n+1}, \lambda^{n+1}) = a_h(\lambda^n, \lambda^n) - 2\rho_n a_h(w^n, \lambda^n) + \rho_n^2 a_h(w^n, w^n). \tag{6.27}$$

The quantities ρ_n and $a_h(w^n, w^n)\, (= \int_\Omega \overline{r}^n w^n \, d\mathbf{x})$ are known. On the other hand the relation

$$a_h(w^n, \lambda^n) = -\int_\Omega \nabla \overline{\psi}^n \cdot \nabla \lambda^n \, d\mathbf{x} + \int_\Omega \overline{\varpi}^n \lambda^n \, d\mathbf{x} \tag{6.28}$$

implies that the second term in the right–hand side of (6.27) is easy to compute. Therefore computing $a_h(\lambda^{n+1}, \lambda^{n+1})$ is also easy if one knows $a_h(\lambda^n, \lambda^n)$, that is (by induction) $a_h(\lambda^0, \lambda^0)$. Actually,

$$a_h(\lambda^0, \lambda^0) = -\int_\Omega \nabla \Psi^0 \cdot \nabla \lambda^0 \, d\mathbf{x} + \int_\Omega \Omega^0 \lambda^0 \, d\mathbf{x} \left(= \int_\Omega |\Omega^0|^2 \, d\mathbf{x} \right), \tag{6.29}$$

where, in (6.29), $\{\Omega^0, \Psi^0\} \in V_h \times V_{0h}$, is uniquely defined by:

$$\begin{cases} \Omega^0 - \lambda^0 \in V_{0h}, \\ \int_\Omega \nabla \Omega^0 \cdot \nabla \varphi \, d\mathbf{x} = 0, \quad \forall \varphi \in V_{0h}, \end{cases} \tag{6.30}$$

$$\begin{cases} \Psi^0 \in V_{0h}, \\ \int_\Omega \nabla \Psi^0 \cdot \nabla \varphi \, d\mathbf{x} = \int_\Omega \Omega^0 \varphi \, d\mathbf{x}, \quad \forall \varphi \in V_{0h}. \end{cases} \tag{6.31}$$

7. Numerical examples

Before we present numerical results, we would like to remember that a possible choice for operator S is given by (4.17), where B depends on the parameter κ, as is shown in (4.14). The following numerical experiments show that a good option is to choose $0 \leq \kappa < 1$.

7.1. **Numerical solution of some bi-harmonic problems with closed form solution.**

We provide closed form solutions to three particular bi-harmonic problems of type (2.4) in the unit disk $\Omega = \left\{(x_1, x_2) \,|\, x_1^2 + x_2^2 < 1\right\}$ and boundary $\Gamma = \partial\Omega$. We take advantage of these problems to validate the methodology we discussed in Sect. 3 to Sect. 6, in particular the conjugate gradient algorithm (6.9)–(6.26). In order to test convergence of the numerical results, three different meshes are considered for the finite element discretization of the elliptical problems that arise in that algorithm: a base mesh M_1, which includes 146 vertices and 258 triangles, with mesh size $h = 0.1$ approximately; M_2 with 549 vertices and 1032 triangles, obtained by a regular refinement of M_1; M_3 with 2129 vertices and 4128 triangles and obtained by a regular refinement of M_2. These meshes are visualized in Figure 1.

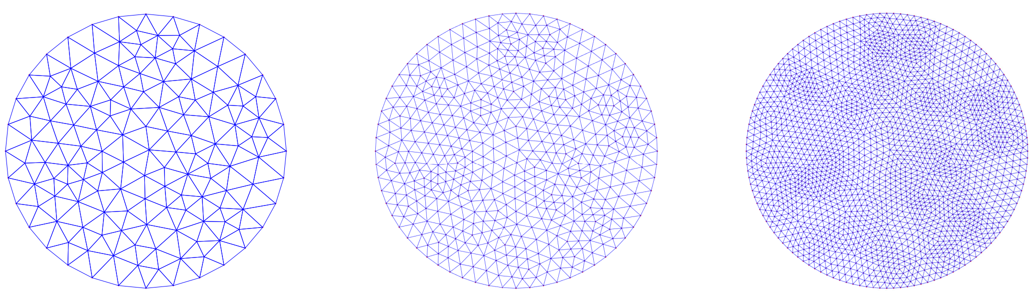

FIGURE 1. Mesh M_1 on a circular domain of radius 1 and its two regular refinements, M_2 and M_3.

Example 7.1. The *first* bi-harmonic problem we consider is the simple one defined by

$$\begin{cases} \Delta^2 \psi = 64 \text{ in } \Omega, \\ \psi = 0 \text{ on } \Gamma, \\ \dfrac{\partial \psi}{\partial n} = 0 \text{ on } \Gamma. \end{cases} \tag{7.1}$$

The unique solution of this problem is given by $\psi(x_1, x_2) = (r^2 - 1)^2, \ \forall (x_1, x_2) \in \overline{\Omega}$, with $r = \sqrt{x_1^2 + x_2^2}$, and compatible function f given by $f(x_1, x_2) = 16r^2 - 8 + \varphi(x_1, x_2)$, where φ is an arbitrary harmonic function.

The numerical results for different values of κ are summarized in Table 1, with $tol = 10^{-5}$ to stop de CG iterations for all cases. In that table, n denotes de number of cg-iterations necessary to obtain the numerical solution ψ_h^n within the given tolerance,

$$\mathrm{Er}(\psi_h^n, \psi) = \|\psi_h^n - \psi\|_{L_2(\Omega)} / \|\psi\|_{L_2(\Omega)}$$

is the relative error, and finally $r_{M1,M2}$, $r_{M2,M3}$ are the numerical rates of convergence. These results show that the numerical method is of order close to two for all values of κ. For smaller values of the stopping parameter tol more iterations are needed to get convergence. Figure 2 shows the numerical solution with mesh M_3.

TABLE 1. Numerical results for problem (7.1) for different values of κ, $tol = 10^{-5}$.

Mesh	M_1		M_2		M_3		Rate of convergence	
κ	n	$\mathrm{Er}(\psi_h^n, \psi)$	n	$\mathrm{Er}(\psi_h^n, \psi)$	n	$\mathrm{Er}(\psi_h^n, \psi)$	$r_{M1,M2}$	$r_{M2,M3}$
0	1	3.9107×10^{-2}	1	9.8778×10^{-3}	1	2.4774×10^{-3}	1.9852	1.9954
10^{-8}	1	3.9107×10^{-2}	1	9.8778×10^{-3}	1	2.4774×10^{-3}	1.9852	1.9954
10^{-4}	1	3.9107×10^{-2}	1	9.8778×10^{-3}	1	2.4774×10^{-3}	1.9852	1.9954
10^{-1}	1	3.9107×10^{-2}	1	9.8778×10^{-3}	1	2.4774×10^{-3}	1.9852	1.9954
10^{0}	9	3.8920×10^{-2}	1	9.8778×10^{-3}	1	2.4774×10^{-3}	1.9783	1.9954
10^{1}	5	3.9146×10^{-2}	1	9.8778×10^{-3}	1	2.4774×10^{-3}	1.9866	2.0311
10^{4}	3	3.9386×10^{-2}	8	1.0168×10^{-2}	9	2.5557×10^{-3}	1.9536	1.9923
10^{8}	3	3.9386×10^{-2}	8	1.0168×10^{-2}	9	2.5557×10^{-3}	1.9536	1.9923

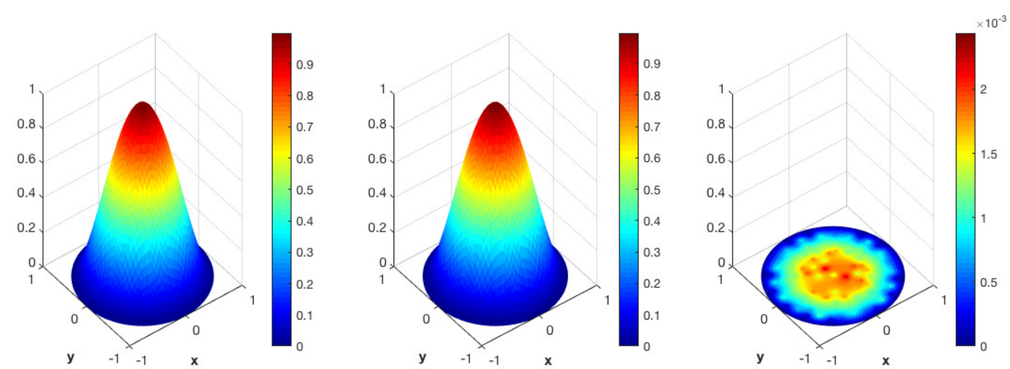

FIGURE 2. Exact solution ψ of problem (7.1) (left), approximated solution ψ_h^n (center) and their difference (right). Mesh M_3, $n = 1$, $\kappa = 10^{-4}$, $tol = 10^{-5}$.

Example 7.2. The *second* bi-harmonic problem we consider reads as

$$\begin{cases} \Delta^2 \psi = 16r^2 e^{r^2}(r^8 + 10r^6 + 23r^4 + 8r^2 - 2) \text{ in } \Omega, \\ \psi = 0 \text{ on } \Gamma, \\ \dfrac{\partial \psi}{\partial n} = 0 \text{ on } \Gamma. \end{cases} \tag{7.2}$$

The unique solution this time is given by $\psi(x_1, x_2) = e^{r^2}(r^2 - 1)^2$, $\forall (x_1, x_2) \in \bar{\Omega}$, and the compatible functions f are given by $f(x_1, x_2) = 4e^{r^2}(r^6 + 3r^4 - r^2 - 1) + \varphi(x_1, x_2)$, φ being an arbitrary harmonic function.

The numerical results are summarized in Table 2, which were again obtained with the same stopping parameter: $tol = 10^{-5}$. These results show a convergence rate of order two when $0 \leq \kappa \leq 10^8$. Figure 3 shows the solution in this case.

TABLE 2. Numerical results for problem (7.2) for different values of κ, $tol = 10^{-5}$.

Mesh	M_1		M_2		M_3		Rate of convergence	
κ	n	$\mathrm{Er}(\psi_h^n, \psi)$	n	$\mathrm{Er}(\psi_h^n, \psi)$	n	$\mathrm{Er}(\psi_h^n, \psi)$	$r_{M1,M2}$	$r_{M2,M3}$
0	5	1.2498×10^{-1}	1	2.2730×10^{-2}	1	5.6235×10^{-3}	2.4590	2.0151
10^{-8}	5	1.2498×10^{-1}	1	2.2730×10^{-2}	1	5.6235×10^{-3}	2.4590	2.0151
10^{-4}	5	1.2485×10^{-1}	1	2.2730×10^{-2}	1	5.6235×10^{-3}	2.4575	2.0151
10^{-1}	5	1.1627×10^{-1}	1	2.2730×10^{-2}	1	5.6235×10^{-3}	2.3548	2.0151
10^{0}	39	2.0335×10^{-1}	1	2.2730×10^{-2}	1	5.6235×10^{-3}	3.1613	2.0151
10^{1}	3	9.2488×10^{-2}	3	2.3069×10^{-2}	1	5.6235×10^{-3}	2.0033	2.0364
10^{4}	3	9.4737×10^{-2}	3	2.3356×10^{-2}	3	5.7783×10^{-3}	2.0201	2.0151
10^{8}	3	9.4739×10^{-2}	3	2.3346×10^{-2}	3	5.7783×10^{-3}	2.0208	2.0146

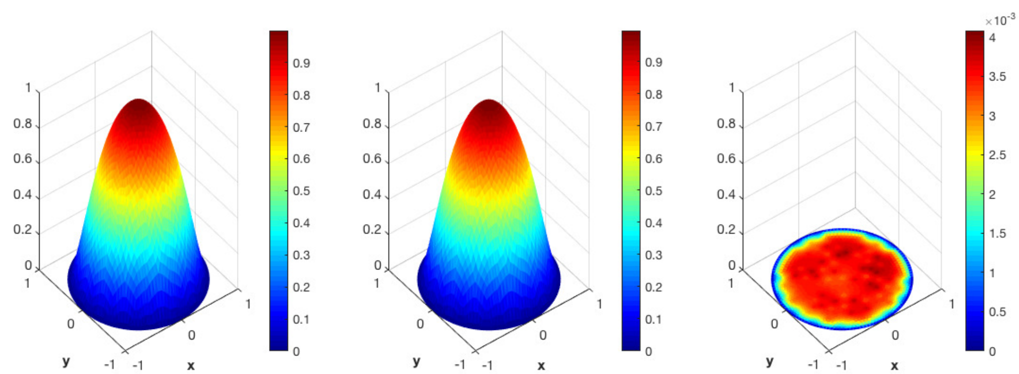

FIGURE 3. Exact solution ψ of problem (7.2) (left), approximated solution ψ_h^n (center) and their difference (right). Mesh M_3, $n = 1$, $\kappa = 10^{-4}$, $tol = 10^{-5}$.

Example 7.3. This problem is more interesting, in some sense. It is defined by

$$\begin{cases} \Delta^2 \psi = 2\pi\delta_{(0,0)} \text{ in } \Omega, \\ \psi = 0 \text{ on } \Gamma, \\ \dfrac{\partial \psi}{\partial n} = 0 \text{ on } \Gamma, \end{cases} \tag{7.3}$$

where $\delta_{(0,0)}$ is the Dirac measure at $(0,0)$. Problem (7.3) has a unique solution in $H_0^2(\Omega)$ given by

$$\psi(x_1,x_2) = r^2 \ln r/4 + (1-r^2)/8, \;\; \forall (x_1,x_2) \in \bar{\Omega},$$

and compatible functions f being given by $f(x_1,x_2) = \ln r + \varphi(x_1,x_2)$, φ being an arbitrary harmonic function.

The numerical results are summarized in Table 3. Those results were obtained with the stopping parameter $tol = 10^{-5}$. For this case second order convergence is attained with the first refinement of mesh M_1, but this rate is lost with the second refinement. We think that the loss of regularity of the solution at the origin explains this behavior. Figure 4 shows the solution ψ_h^n for $\kappa = 10^{-4}$ with the mesh M_3.

TABLE 3. Numerical results for problem (7.3) for different values of κ, $tol = 10^{-5}$.

Mesh	M_1		M_2		M_3		Rate of convergence	
κ	n	$\mathrm{Er}(\psi_h^n,\psi)$	n	$\mathrm{Er}(\psi_h^n,\psi)$	n	$\mathrm{Er}(\psi_h^n,\psi)$	$r_{M1,M2}$	$r_{M2,M3}$
0	1	2.3571×10^{-2}	1	5.8149×10^{-3}	1	3.1579×10^{-3}	2.0192	0.8808
10^{-8}	1	2.3571×10^{-2}	1	5.8149×10^{-3}	1	3.1579×10^{-3}	2.0192	0.8808
10^{-4}	1	2.3571×10^{-2}	1	5.8149×10^{-3}	1	3.1579×10^{-3}	2.0192	0.8808
10^{-1}	1	2.3571×10^{-2}	1	5.8149×10^{-3}	1	3.1579×10^{-3}	2.0192	0.8808
10^{0}	1	2.3571×10^{-2}	1	5.8149×10^{-3}	1	3.1579×10^{-3}	2.0192	0.8808
10^{1}	1	2.3571×10^{-2}	1	5.8149×10^{-3}	1	3.1579×10^{-3}	2.0192	0.8808
10^{4}	12	2.3361×10^{-2}	1	5.8149×10^{-3}	1	3.1579×10^{-3}	2.0063	0.8808
10^{8}	12	2.3361×10^{-2}	5	6.0156×10^{-3}	6	3.2054×10^{-3}	1.9573	0.9082

For this example we present the following table, where we show the numerical errors obtained with the H^1 semi-norm instead of the L_2 norm.

TABLE 4. Numerical results for problem (7.3) for different values of κ, $tol = 10^{-5}$, where the relative errors are calculated with the H^1 semi-norm.

Mesh	$M_1(723, 1349)$		$M_2(2794, 5396)$		$M_3(10983, 21584)$		Rate of convergence	
κ	n	$\mathrm{Er}(\psi_h^n, \psi)_{H^1(\Omega)}$	n	$\mathrm{Er}(\psi_h^n, \psi)_{H^1(\Omega)}$	n	$\mathrm{Er}(\psi_h^n, \psi)_{H^1(\Omega)}$	$r_{M1,M2}$	$r_{M2,M3}$
0	1	3.7868×10^{-2}	1	1.0114×10^{-2}	1	4.5706×10^{-3}	1.9046	1.1459
10^{-8}	1	3.7868×10^{-2}	1	1.0114×10^{-2}	1	4.5706×10^{-3}	1.9046	1.1459
10^{-4}	1	3.7868×10^{-2}	1	1.0114×10^{-2}	1	4.5706×10^{-3}	1.9046	1.1459
10^{-1}	1	3.7868×10^{-2}	1	1.0114×10^{-2}	1	4.5706×10^{-3}	1.9046	1.1459
10^{0}	1	3.7868×10^{-2}	1	1.0114×10^{-2}	1	4.5706×10^{-3}	1.9046	1.1459
10^{1}	1	3.7868×10^{-2}	1	1.0114×10^{-2}	1	4.5706×10^{-3}	1.9046	1.1459
10^{4}	12	3.7432×10^{-2}	1	1.0114×10^{-2}	1	4.5706×10^{-3}	1.8879	1.1459
10^{8}	12	3.7432×10^{-2}	5	1.0114×10^{-2}	6	4.5889×10^{-3}	1.8879	1.1401

The relative errors obtained with the H^1 semi-norm are slightly higher than those obtained with the L_2 norm, but there is a improvement on the rate of convergence for the second refinement of the mesh, as show in the last column of Table 4. However, we are not able to elucidate new relevant information from this table. As we have already said before, the low rate of convergence with the second refinement is due to the loss of regularity of the solution at the origin.

Figure 4 illustrates the exact and approximated solution obtained with $\kappa = 10^{-4}$.

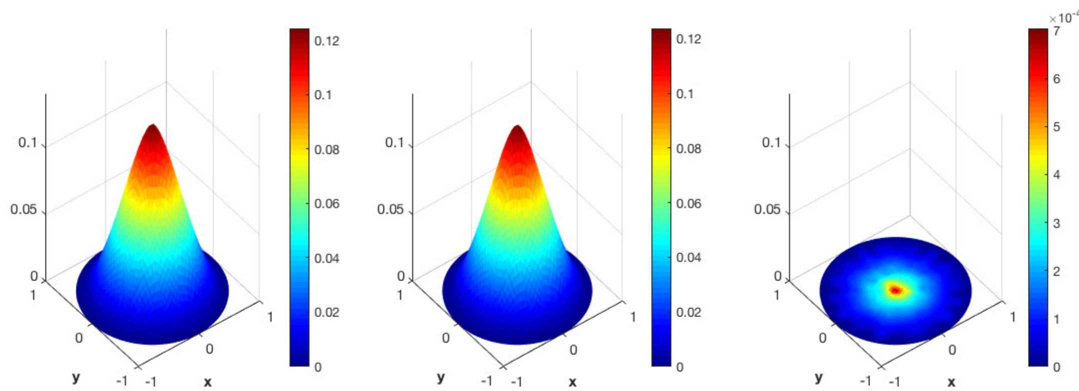

FIGURE 4. Exact solution ψ of problem (7.3) (left), approximated solution ψ_h^n (center) and their difference (right). Mesh M_3, $n = 1$, (right), $\kappa = 10^{-4}$, $tol = 10^{-5}$.

7.2. **Numerical results for a 2D complex region.** Here we consider a non circular 2D complex region as computational domain. Like in the previous examples, for the numerical experiments we discretize this domain with triangular elements and consider three different meshes, which we will still call M_1, M_2 and M_3, each one is obtained as a regular refinement of the previous one, as shown in Figure 5.

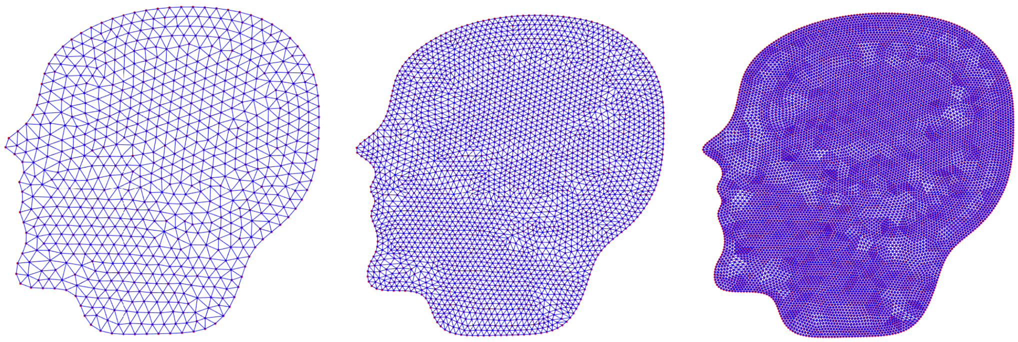

FIGURE 5. Mesh M_1 on a complex domain, with 723 vertices and 1349 triangles, and its two regular refinements: M_2 with 2794 vertices and 5396 triangles, M_3 with 10983 vertices and 21584 triangles.

Example 7.4. We consider the function

$$f(x,y) = e^{-[(x-x_0)^2+(y-y_0)^2]/2\beta^2} \left\{ -\frac{2}{\beta^2} + \frac{1}{\beta^4} \left[(x-x_0)^2 + (y-y_0)^2 \right] \right\}, \tag{7.4}$$

where (x_0, y_0) is a point in Ω and $\beta^2 > 0$ is a small postive constant. The following function

$$\psi(x,y) = e^{-[(x-x_0)^2+(y-y_0)^2)]/2\beta^2}, \quad (x,y) \in \Omega, \tag{7.5}$$

is a very close approximation to the solution of the bi-harmonic problem (2.4). Although, this function satisfies the differential equation, it does not satisfy exactly the homogeneous boundary conditions; however, both this function and its normal derivative almost vanish at the boundary if (x_0, y_0) is a point in Ω far enough from its boundary Γ, due to the rapid decay of the exponential function as (x,y) moves away from (x_0, y_0). Therefore, for the next numerical experiments we will compute the relative error using this function instead of the exact solution of the biharmonic problem (2.4), where we consider the compatible function $f(x,y)$ given by (7.4).

Next, we consider two numerical examples: one for $\beta^2 = 0.05$ and the other for $\beta^2 = 0.02$. For these examples we will pick the point $(x_0, y_0) = (0.3767, 0.6087)$.

Numerical results for $\beta^2 = 0.05$.

The numerical results are summarized in Table 5 for different values of the parameter κ. This time the stopping parameter is fixed at $tol = 10^{-5}$ for all cases. We observe, that the errors decrease with each mesh for each case, obtaining second order numerical convergence for $0 \le \kappa \le 10^8$. Figure 6 shows the approximate solution ψ_h^n for $\kappa = 10^{-4}$ obtained with the mesh M_3.

TABLE 5. Numerical results for different values of κ, $tol = 10^{-5}$, $\beta^2 = 0.05$, complex domain.

Mesh	$M_1(723,1349)$		$M_2(2794,5396)$		$M_3(10983,21584)$		Rate of convergence	
κ	n	$\mathrm{Er}(\psi_h^n,\psi)$	n	$\mathrm{Er}(\psi_h^n,\psi)$	n	$\mathrm{Er}(\psi_h^n,\psi)$	$r_{M1,M2}$	$r_{M2,M3}$
0	1	1.8881×10^{-2}	1	4.8150×10^{-3}	1	1.1823×10^{-3}	1.9713	2.0259
10^{-8}	1	1.8881×10^{-2}	1	4.8150×10^{-3}	1	1.1823×10^{-3}	1.9713	2.0259
10^{-4}	1	1.8881×10^{-2}	1	4.8150×10^{-3}	1	1.1823×10^{-3}	1.9713	2.0259
10^{-1}	1	1.8881×10^{-2}	1	4.8150×10^{-3}	1	1.1823×10^{-3}	1.9713	2.0259
10^{0}	1	1.8881×10^{-2}	1	4.8150×10^{-3}	1	1.1823×10^{-3}	1.9713	2.0259
10^{1}	1	1.8881×10^{-2}	1	4.8150×10^{-3}	1	1.1823×10^{-3}	1.9713	2.0259
10^{4}	9	1.7464×10^{-2}	1	4.8150×10^{-3}	1	1.1823×10^{-3}	1.8588	2.0259
10^{8}	9	1.7464×10^{-2}	9	4.6631×10^{-3}	2	1.6674×10^{-3}	1.9050	0.4466

For this case we also computed the relative errors with the H^1 semi-norm, which again are slightly higher than those obtained with the L_2 norm. We decided no to include a complete table again, but only we want to say that converge rates are approximately 1.92 for the first refinement and 1.95 for the second refinement.

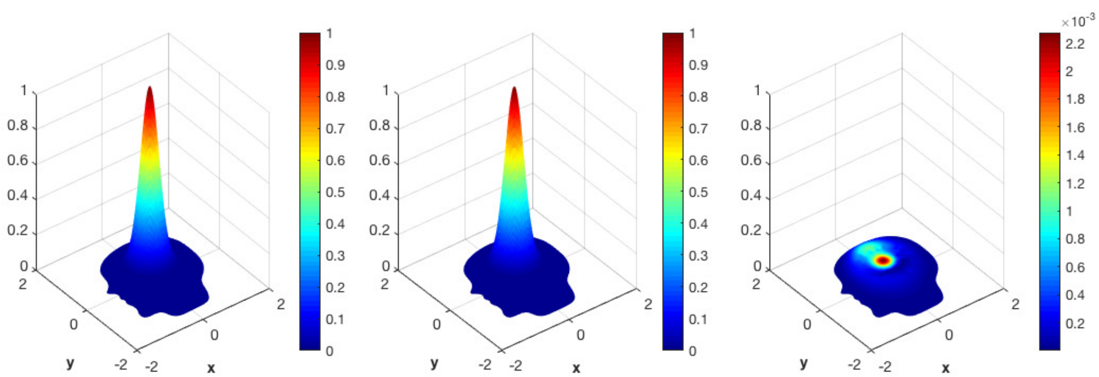

FIGURE 6. Graph of exact solution ψ (left), approximate solution ψ_h^n (center) and their difference (right). Mesh M_3, $n = 1$, $\kappa = 10^{-4}$, $tol = 10^{-5}$, $(x_0,y_0) = (0.3767,0.6087)$, $\beta^2 = 0.05$.

Numerical results for $\beta^2 = 0.02$

These results are summarized in Table 6 for different values of κ, where the stopping criterion is again fixed at $tol = 10^{-5}$. Figure 7 shows the exact and approximate solutions, the last one obtained with the mesh M_3 and $\kappa = 10^{-4}$.

This time we obtain a slight loss of precision in the numerical results (and of the order of convergence), when compared with the numerical results of the previous example. We believe that this loss of accuracy is due to the lack of resolution around the region where the 'spike' of the solution appears, since the same meshes are used to compute the numerical solutions for both cases, $\beta^2 = 0.05$ and $\beta^2 = 0.02$.

TABLE 6. Numerical results for different values of κ, $tol = 10^{-5}$, $\beta^2 = 0.02$, complex domain.

Mesh	$M_1(723, 1349)$		$M_2(2794, 5396)$		$M_3(10983, 21584)$		Rate of convergence	
κ	n	$\mathrm{Er}(\psi_h^n, \psi)$	n	$\mathrm{Er}(\psi_h^n, \psi)$	n	$\mathrm{Er}(\psi_h^n, \psi)$	$r_{M1,M2}$	$r_{M2,M3}$
0	1	3.9538×10^{-2}	1	1.0668×10^{-2}	1	2.7217×10^{-3}	1.8900	1.9707
10^{-8}	1	3.9538×10^{-2}	1	1.0668×10^{-2}	1	2.7217×10^{-3}	1.8900	1.9707
10^{-4}	1	3.9538×10^{-2}	1	1.0668×10^{-2}	1	2.7217×10^{-3}	1.8900	1.9707
10^{-1}	1	3.9538×10^{-2}	1	1.0668×10^{-2}	1	2.7217×10^{-3}	1.8900	1.9707
10^{0}	1	3.9538×10^{-2}	1	1.0668×10^{-2}	1	2.7217×10^{-3}	1.8900	1.9707
10^{1}	1	3.9538×10^{-2}	1	1.0668×10^{-2}	1	2.7217×10^{-3}	1.8900	1.9707
10^{4}	1	3.9538×10^{-2}	1	1.0668×10^{-2}	1	2.7217×10^{-3}	1.8900	1.9707
10^{8}	101	3.9163×10^{-2}	9	1.0612×10^{-2}	1	2.7217×10^{-3}	1.8838	1.9631

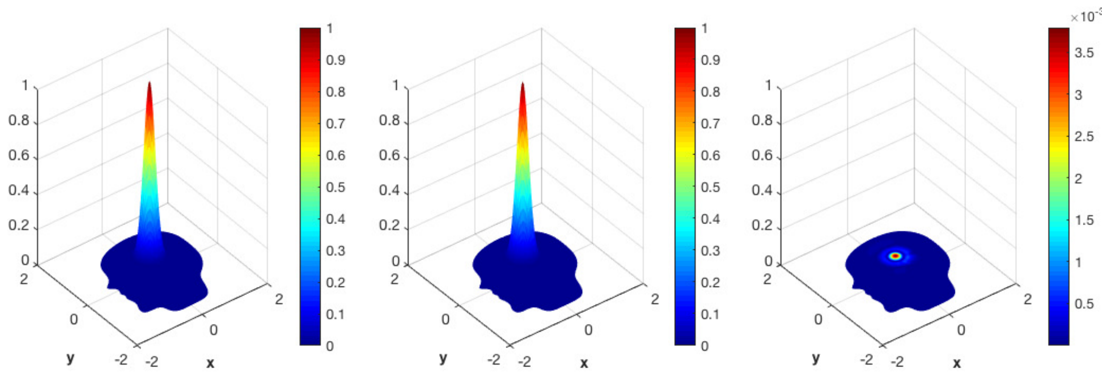

FIGURE 7. Graph of exact solution ψ (left), approximate solution ψ_h^n (center) and their difference (right). Mesh M_3, $n = 1$, $\kappa = 10^{-4}$, $tol = 10^{-5}$, $(x_0, y_0) = (0.3767, 0.6087)$, $\beta^2 = 0.02$.

8. CONCLUSIONS

We solved numerically a linear bi-harmonic problem, which arises when solving inverse problems in electro-encephalography, using low order Lagrange finite element approximations. We reformulate the problem as a functional equation associated with a linear boundary operator of the Steklov-Poincare type, for which we apply a conjugate gradient algorithm that requires the solution of some few second-order elliptic equations per iteration. The numerical experiments we performed show that this method is efficient and accurate for the given bi-harmonic problem defined in simple and complex 2D domains. We can claim that the method is second order accurate, unless the resolution of the mesh does does not capture high gradients, but even for this case accurate solutions are obtained.

Acknowledgements

The authors want to express our gratitude to R. Glowinski for his interest in the inverse electroencephalographic problem. This work revels our most recent collaboration with him and we decided to finish it in order to seek its publication in the special issue dedicated to his 85th birthday (now unfortunately post-mortem). Likewise, the third author wishes to thank the support of the UAM-Iztapalapa graduate math program.

REFERENCES

[1] A.A. Abushama, B. Bialecki, Modified nodal cubic spline collocation for biharmonic equations, Numerical Algorithms 43 (2006) 331-353.

[2] M. Arad, A. Yakhot, G. Ben-Dor, A highly accurate numerical solution of a biharmonic equation, Numerical Methods for Partial Differential Equations: An International Journal 13 (1997) 375-391.

[3] A. El Badia, T. Ha Duong, Some remarks on the problem of source identification from boundary measurements, Inverse Problems 14 (1998) 883-891.

[4] B. Bialecki, A fast solver for the orthogonal spline collocation solution of the biharmonic Dirichlet problem on rectangles, Journal of Computational Physics 191 (2003) 601-621.

[5] B. Bialecki, G. Fairweather, A. Karageorghis, J. Maack, A quadratic spline collocation method for the Dirichlet biharmonic problem, Numerical Algorithms 83 (2020) 165-199.

[6] Bjørstad, P. Fast numerical solution of the biharmonic Dirichlet problem on rectangles, SIAM Journal on Numerical Analysis 20 (1983) 59-71.

[7] B. L. Buzbee, F. W. Dorr, The direct solution of the biharmonic equation on rectangular regions and the Poisson equation on irregular regions, SIAM Journal on Numerical Analysis 11 (1974) 753-763.

[8] G. Chen, Z. Li, P. Lin, A fast finite difference method for biharmonic equations on irregular domains and its application to an incompressible Stokes flow, Advances in Computational Mathematics 29 (2008) 113-133.

[9] X. L. Cheng, W. Han, H.C. Huang, Some mixed finite element methods for biharmonic equation, Journal of Computational and Applied Mathematics 126 (2000) 91-109.

[10] S. Christiansen, P. Hougaard, An investigation of a pair of integral equations for the biharmonic problem, IMA Journal of Applied Mathematics 22 (1978) 15-27.

[11] S. Christiansen, Derivation and analytical investigation of three direct boundary integral equations for the fundamental biharmonic problem, Journal of computational and applied mathematics 91 (1998) 231-247.

[12] P. G. Ciarlet, P. A. Raviart, A mixed finite element method for the biharmonic equation, In: C. De Boor (ed.) Mathematical aspects of finite elements in partial differential equations, pp. 125-145, Academic Press, New York, 1974.

[13] B. Cockburn, B. Dong, J. Guzmán, A hybridizable and superconvergent discontinuous Galerkin method for biharmonic problems, Journal of Scientific Computing 40 (2009) 141-187.

[14] M. Costabel, J. Saranen, Boundary element analysis of a direct method for the biharmonic Dirichlet problem. In: Dym, H., Goldberg, S., Kaashoek, M.A., Lancaster, P. (eds.) The Gohberg Anniversary Collection. Operator Theory: Advances and Applications, vol 41, pp. 569-587, Birkhäuser, Basel, 1989.

[15] J.J. Conde-Mones, El problema inverso electroencefalográfico para fuentes volumétricas y su desarrollo numérico en geometrías simples, PhD. thesis, 2013.

[16] C. Davini, I. Pitacco, An unconstrained mixed method for the biharmonic problem, SIAM Journal on Numerical Analysis 38 (2000) 820-836.

[17] J.C. De Munck, B.W. Van Dijk, H. Spekreijse, Mathematical dipoles are adequate to describe realistic generators of human brain activity, IEEE Transactions Biomedical Engineering 35 (1988) 960-966.

[18] L.W. Ehrlich, M.M. Gupta, Some difference schemes for the biharmonic equation, SIAM Journal on Numerical Analysis 12 (1975) 773-790.

[19] B. Fuglede, On a direct method of integral equations for solving the biharmonic Dirichlet problem, ZAMM Journal of Applied Mathematics and Mechanics / Zeitschrift für Angewandte Mathematik und Mechanik 61 (1981) 449-459.

[20] R. Glowinski, Finite element methods for incompressible viscous flow, Handbook of Numerical Analysis, vol. 9, North-Holland, Amsterdam, 2003.

[21] R. Glowinski, Variational Methods for the Numerical Solution of Nonlinear Elliptic Problems, SIAM, Philadelphia, 2015.

[22] R. Glowinski, J. L. Lions, J. He, Exact and approximate controllability for distributed parameter systems: A Numerical Approach, Encyclopedia of Mathematics and its Applications 117, Cambridge University Press, 2008.

[23] R. Glowinski, O. Pironneau, Numerical methods for the first bi-harmonic equation and for the two-dimensional Stokes problem, SIAM Review 21 (1979) 167-212.

[24] A. Greenbaum, L. Greengard, A. Mayo, On the numerical solution of the biharmonic equation in the plane, Physica D: Nonlinear Phenomena 60 (1992) 216-225.

[25] S. Huang, Y.J. Liu, A fast multipole boundary element method for solving the thin plate bending problem, Engineering Analysis with Boundary Elements 37 (2013) 967-976.

[26] Y. Jeon, An indirect boundary integral equation method for the biharmonic equation, SIAM journal on numerical analysis 31 (1994) 461-476.

[27] Y. Jiang, B. Wang, Y. Xu, A Fast Fourier–Galerkin Method Solving a Boundary Integral Equation for the Biharmonic Equation, SIAM Journal on Numerical Analysis 52 (2014) 2530-2554.

[28] M.C. Lai, H.C. Liu, Fast direct solver for the biharmonic equation on a disk and its application to incompressible flows, Applied Mathematics and Computation 164 (2005) 679-695.

[29] A. Lopez-Rincon, S. Shimoda, The inverse problem in electroencephalography using the bidomain model of electrical activity, Journal of Neuroscience Methods 274 (2016) 94-105.

[30] M.M. Morín-Castillo, J. Arriaga-Hernández, B. Cuevas-Otahola, J. J. Oliveros-Oliveros, Analysis of Dipolar Sources in the Solution of the Electroencephalographic Inverse Problem, Mathematics 10 (2022) 1926.

[31] M. M. Morín, C. Netzahualcoyotl, J. J. Oliveros, J. J. Conde and L.H. Juárez, Stable identification of sources located on separation interfaces of two different homogeneous media, Advances in Differential Equations and Control Processes, 20 (2019) 53-97.

[32] L. Mu, J. Wang, Y. Wang, X. Ye, A weak Galerkin mixed finite element method for biharmonic equations, In: O.P. Iliev, S.D. Margenov, P.D. Minev, P.S. Vassilevski, L.T. Zikatanov (eds.) Numerical Solution of Partial Differential Equations: Theory, Algorithms, and Their Applications, pp. 247-277, Springer, New York, 2013.

[33] L. Mu, J. Wang, X. Ye, Weak Galerkin finite element methods for the biharmonic equation on polytopal meshes, Numerical Methods for Partial Differential Equations 30 (2014) 1003-1029.

[34] J. Nečas, Direct Methods in the Theory of Elliptic Equations, Springer monographs in mathematics, 2012.

[35] J. Oliveros, M. Morín, J. Conde, A. Fraguela, A regularization strategy for the inverse problem of identification of bioelectrical sources for the case of concentric spheres. Far East Journal of Applied Mathematics 77 (2013) 1-20.

[36] J.W. Stephenson, Single cell discretizations of order two and four for biharmonic problems, Journal of Computational Physics, 55 (1984) 65-80.

[37] Y. Xie, W. Ying, W.C. Wang, A High-Order Kernel-Free Boundary Integral Method for the Biharmonic Equation on Irregular Domains, Journal of Scientific Computing 80 (2019) 1681-1699.

[38] R. Zhang, Q. Zhai, A weak Galerkin finite element scheme for the biharmonic equations by using polynomials of reduced order, Journal of Scientific Computing 64 (2015) 559-585.